Defect Healing and Enhanced Nucleation of Carbon Nanotubes by Low-Energy Ion Bombardment

E. C. Neyts,[1,*] K. Ostrikov,[2] Z. J. Han,[2] S. Kumar,[2] A. C. T. van Duin,[3] and A. Bogaerts[1]

[1]*University of Antwerp, Department of Chemistry, PLASMANT Research Group, 2610 Wilrijk-Antwerp, Belgium*

[2]*Commonwealth Scientific and Industrial Research Organisation, Materials Science and Engineering, Plasma Nanoscience Center Australia (PNCA), P.O. Box 218, Lindfield NSW 2070, Australia*

[3]*Pennsylvania State University, Department of Mechanical and Nuclear Engineering, University Park, Pennsylvania 16802, USA*

(Received 7 November 2012; published 5 February 2013)

Structural defects inevitably appear during the nucleation event that determines the structure and properties of single-walled carbon nanotubes. By combining ion bombardment experiments with atomistic simulations we reveal that ion bombardment in a suitable energy range allows these defects to be healed resulting in an enhanced nucleation of the carbon nanotube cap. The enhanced growth of the nanotube cap is explained by a nonthermal ion-induced graphene network restructuring mechanism.

DOI: 10.1103/PhysRevLett.110.065501 PACS numbers: 61.80.−x, 31.15.xv, 61.48.De, 68.35.Dv

Despite more than 20 years of research, the problem of structure, and, in particular, chirality control of single-walled carbon nanotubes (SWCNTs) has not been solved [1–6]. This is intimately connected to the occurrence of structural defects that inevitably appear during the nucleation event of the SWCNT [7,8]. This current lack of structural control severely impedes the exceptional promise of the SWCNTs to materialize in the next-generation nanodevices, which demand defect-free SWCNTs with precisely controlled sizes and atomic structure [9,10]. In addition to growth rate driven chirality control [11,12] and selective etching [13], it has often been suggested that control over the tube structure can be accomplished by control over this nucleation event, which can be achieved if the catalyst nanoparticle (CNP) remains solid so that the lattices of SWCNT and CNP could match [14–18]. Because of the intrinsically random nature of impingement, diffusion, and segregation processes, defects are inevitably formed, especially at lower temperatures that are essential to keep the CNP solid [7].

Thermal healing of defects requires high temperatures [19], which in turn inevitably cause melting of the CNP due to the Gibbs-Thomson effect and thus any solid catalyst template effect is lost [20]. Thus, nonthermal defect healing is crucial, which, however, has not yet been achieved. Here we present evidence that such nonthermal defect healing may be accomplished by using ion bombardment, which is frequently used for removing and (intentionally) damaging material [21,22], e.g., sputtering in plasma and ion-assisted processes. While ion bombardment is indeed typically considered detrimental in CNT growth, leading to defect creation instead of defect healing [23], it should be noted that in other systems low-energy bombardment has also proven to be beneficial, e.g., ion-induced stress release in covalent solids [24] or epitaxial growth of cubic boron nitride on diamond [25].

To confirm the intrinsic defect healing ability of ion bombardment in CNT growth, we performed both experiments and reactive molecular dynamics (MD or RMD) simulations of ion bombardment on growing SWCNTs. Both MD simulations and experiments suggest that defects can be healed nonthermally and nucleation can be enhanced if the ion energy is selected in the proper range. As will be demonstrated below, this agreement is quantitative and is obtained under the same values of process temperature and ion energy. This possibility opens new avenues for the effective nonthermal control over SWCNT growth that may contribute to solving the ultimate challenge of chirality control.

The initial structure for the simulations is a previously generated nascent defected SWCNT cap, which was grown during our previous simulations of electric field enhanced SWCNT growth on a ~1 nm surface bound Ni_{40} cluster [26]. The cluster is thermalized at 1000 K employing the Berendsen heat bath with a coupling constant of 100 fs [27]. This structure is bombarded with Ar atoms having an energy in the range of 5–50 eV, with 5 eV steps. Thus, 10 cases were investigated, corresponding to 10 different Ar energies. Each of these cases was repeated 10 times to gather statistics. In each case, the total number of consecutive Ar impacts was set to 200. Thus, the total simulation set consists of 100×200 simulated Ar impacts. In our simulation, we used Ar atoms to represent Ar^+ ions. Indeed, when an ion impinges, it is neutralized by Auger emission, thus effectively resulting in a fast neutral species impinging on the cluster.

C-C, C-Ni, and Ni-Ni interactions were treated using the ReaxFF potential. ReaxFF is based on the concept of a bond order, which is determined by the local environment of each atom [28]. As a reactive potential, it is not constrained to a predefined set of atomic bonds but allows bond formation and bond breaking as the simulation progresses. Besides short ranged interactions, ReaxFF also includes Coulomb and van der Waals interactions, thus enabling the accurate description of covalent, metallic,

and ionic interactions, as well as chemisorption and physisorption processes. Previous simulations employing this force field indicate that ReaxFF is sufficiently accurate to capture all essential processes relevant for CNT growth [8,26,29]. The Ar-C and Ar-Ni interactions were taken into account by a purely repulsive Molière pair potential using Firsov constants [30].

Each Ar impact on the Ni/C structure was followed for 2 ps, using a time step of 0.1 fs. The first 1.6 ps of each impact was followed in the microcanonical ensemble, to mimic an isolated system. The excess heat generated by the impact of the energetic Ar atom was subsequently allowed to dissipate by coupling a heat bath to the system during the remaining 0.4 ps. Throughout the entire simulation, it was ensured that after each impact, the cluster was rethermalized to 1000 K before initiating a new Ar impact. Hence, while during the impacts the ions transfer a considerable amount of energy to the cluster, none of this energy remains in the cluster.

It should be realized that all observed processes are purely due to the short time scale Ar impacts, and not due to long time scale events. In the simulations, the Ar ions impinge normal to the surface, corresponding to the substrate bias accelerated bombardment perpendicular to the substrate in the experiments. Before the impact, the z position of the ion is 10 Å, i.e., beyond the cutoff of the potential. The initial $\{x, y\}$ positions of the impinging particles are randomized, in a circle with a diameter corresponding to the $\{x, y\}$ projection of the target cluster plus 2 Å. This ensures that every initiated ion impact leads to an impingement, but not necessarily on top of the cluster.

To mimic this simulation condition, we customized the experimental pattern of Ni catalyst nanoparticles to have an average diameter of ~1.4–1.5 nm and a size distribution in the range 1–3 nm. This was achieved by thermal fragmentation of a 0.5-nm-thick continuous Ni film deposited by e-beam evaporation onto a Si substrate with a 500-nm-thick thermally grown oxide layer.

To mimic the growth temperature used in the simulation (1000 K or 727 °C), the growth of the short nanotubes and their ion bombardment were performed at temperatures as close as possible to the above simulation temperature, yet still sufficient to grow the single-walled nanotubes. These temperatures were only slightly higher (~730–740 °C).

The SWCNTs were grown on the above pattern of nickel catalyst nanoparticles by using an ethylene hydrocarbon precursor, because this precursor was best suited to produce SWCNTs on Ni catalyst nanoparticles within the required temperature range [31]. The growth times (10, 30, and 60 s) were also chosen deterministically to ensure that single-walled nanotubes emerge and can be identified as such by Raman spectroscopy and scanning electron microscopy. After stopping carbon material supply at 10 s, 30 s, or 60 s, the Ar plasma was turned on, without any bias, and with −20 V and −50 V bias to see the effect of ion bombardment.

Interestingly, there is a remarkable correspondence between the trends observed in the MD simulations and real ion bombardment experiments. In the simulations, the extent of the carbon network is enhanced and the nucleation of the cap is promoted when applying a beam of Ar ions in a narrow energy window of 10–25 eV. Using higher Ar ion energies, the carbon network is destroyed. Also, bombardment of a more developed cap or a growing tube is found to be always detrimental. Experimentally, the structural quality of the graphitic carbon network produced on Ni catalyst nanoparticles after 10 s growth improved when a bias of −20 V was used. The quality of the SWCNT structure decreased when a bias of −50 V was applied. When we bombarded the (still short but already clearly single-walled) nanotubes grown for 30 s, any bombardment was detrimental.

In Fig. 1(a), representative examples in top view and side view are shown of the effect of Ar impacts on the initial cluster, showing that the extent of the carbon network is increased due to the Ar bombardment with energies between 15 and 25 eV. Importantly, while the initial structure contains a relatively high number of defects and carbon atoms not connected in stable ring configurations, most of these defects are eliminated by the bombardment and new stable rings are created. In the particular case shown in the figure (corresponding to 15 eV bombardment), the total number of pentagons in the structure increased from 6 to 10, the number of hexagons increased from 5 to 9, and the number of heptagons increased from 1 to 2, due to the ion bombardment.

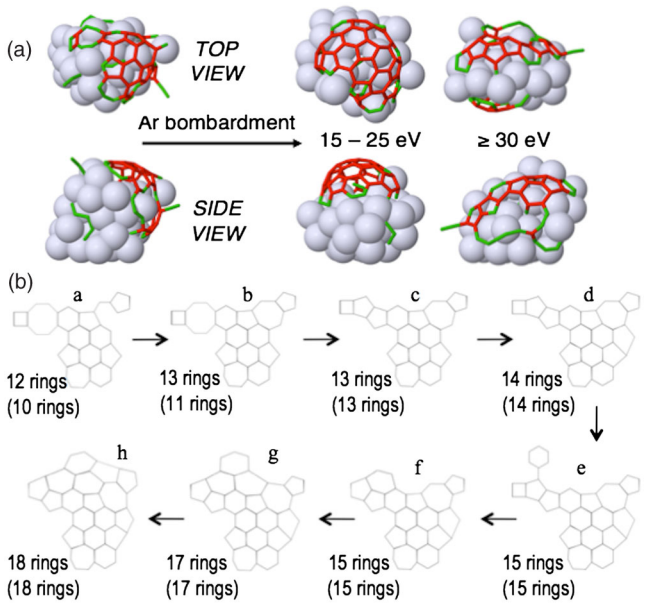

FIG. 1 (color online). (a) Observed defect healing and enhanced cap formation by ion bombardment in the energy range 15–25 eV and destruction of the network at higher energies (>30 eV). (b) Growth of the carbon network due to the ion bombardment at 15 eV, as seen in the MD simulations. The numbers in parentheses indicate the sum of the pentagons, hexagons, and heptagons; the other numbers indicate the total number of rings in the patch.

Thus, overall, 9 new rings were created, while 2 unstable rings (i.e., a square and an octagon) were removed.

In Fig. 1(b), a schematic representation of the evolution of the carbon network is shown for the same structure. The number of pentagons, hexagons, and heptagons in the cap increases from 10 to 18. In the entire structure (i.e., including the cap as well as a few isolated rings on the surface), the total number of rings rises from 14 to 21 (+50%), and the number of pentagons, hexagons, and heptagons increases from 12 to 21 (+75%).

The structural changes as induced by the ion bombardment indicate that a higher quality network is formed. A detailed discussion on these structural changes can be found in the Supplemental Material [32]. When using ion energies equal to or above 30 eV, the cap structure is inevitably damaged, as evidenced by a decreasing number of rings, seen from Fig. 1(a).

In Fig. 2, the average evolution of the number of rings in the cap (counted as the sum of pentagons, hexagons, and heptagons) is shown as a function of the number of Ar impacts, for various impact energies. Three different energy regimes can be discerned.

At low- and medium-impact energies (up to about 25 eV), the extent of the network increases upon ion bombardment. As can be seen in the figure, the influence of the Ar bombardment on the carbon network is rather limited for the lowest impact energy (5 eV), increasing the number of rings on average with 16%. Increasing the energy to 15 eV, however, leads to a substantial rise of 50% in the number of rings. When the Ar impact energy rises further to medium high values of about 30–35 eV, the number of rings remains constant, but the network becomes more disordered and more defected. Thus, our simulations predict that 30–35 eV is the threshold energy below which ion bombardement is beneficial, and above

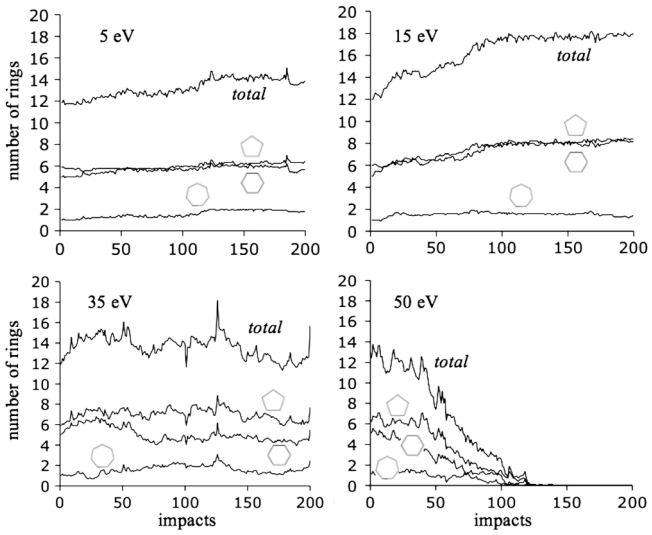

FIG. 2. Evolution of the average number of rings in the carbon network as a function of the number of consecutive Ar impacts, for 4 different impact energies, averaged over 10 independent runs.

which ion bombardment becomes destructive. It can indeed be seen in Fig. 2 that at an Ar ion energy of 50 eV, the cap structure is very quickly destroyed.

The above simulation results are corroborated by the experimental observations. In the experiments, SWCNTs started to appear after 30 s growth time [Figs. 3(a)–3(d)]. Despite of lack of exact time resolution, and given that under similar conditions the incubation time of SWCNTs is typically 5–10 s [3,20], this indicated that the transition from the nucleation to the growth stage occurred most likely between 10 and 30 s. When subjecting to Ar^+ ion bombardment, the Raman G peak of 10 s growth (no nanotubes but likely only developed caps; see energy-dispersive x-ray (EDX) spectra in the Supplemental Material [32]) showed no difference at 0 V bias, but a significant increase in intensity at −20 V bias [Fig. 3(e)]. As the bias was increased to −50 V, detrimental effects appeared on these graphitic structures as evidenced by the disappearance of the graphitic G peak [see also Fig. 3(e)]. In contrast, ion bombardment was always detrimental to 30 s grown tubes even at 0 V biases [Fig. 3(f)].

These transformations in the carbon network are explained by the combined action of a number of processes, i.e., ring formation due to knock-on collisions, collision-induced displacement of C atoms, collision-induced removal of C atoms (i.e., sputtering), and collision-induced cleavage of C-C bonds (see movies in the Supplemental Material [32]).

When an Ar ion impinges on a C atom, up to 71% of its kinetic energy can be transferred to the C atom, based on the mass transfer factor. In a perfect graphene lattice the C-displacement energy has been determined to be in the range 14–32 eV [33–36]. Thus, to destroy such a lattice requires an Ar impact energy in the order of 20–45 eV. However, the growing cap in our simulations is defected, and not all C atoms are fully coordinated. Thus, a lower Ar-impact energy can be expected to displace or eject undercoordinated C atoms from the cap. Based on a binding energy of a one-coordinated C atom of about 6.5 eV, an Ar impact energy of about 10–15 eV may thus already be sufficient for first C displacements. This energy corresponds indeed to the lower threshold energy for observing a beneficial effect of the ion bombardment in both our simulations and experiments. In contrast, at an impact energy of 40 eV or above, all C atoms can easily be removed from the network.

In summary, a number of processes are observed, some of which enhance the network formation, while some of them destroy the network. Clearly, at medium low energies, up to about 25 eV, the network enhancing processes are dominant, and enhance the growth of a CNT. From about 35 eV, however, the destructive events dominate and prevent the growth of a CNT. Thus, by carefully adjusting the bias, the ion (peak) energy can be controlled, and therefore a control over the network formation can be obtained.

Although we did not measure the ion energy distribution function, we can estimate the peak energy for a given

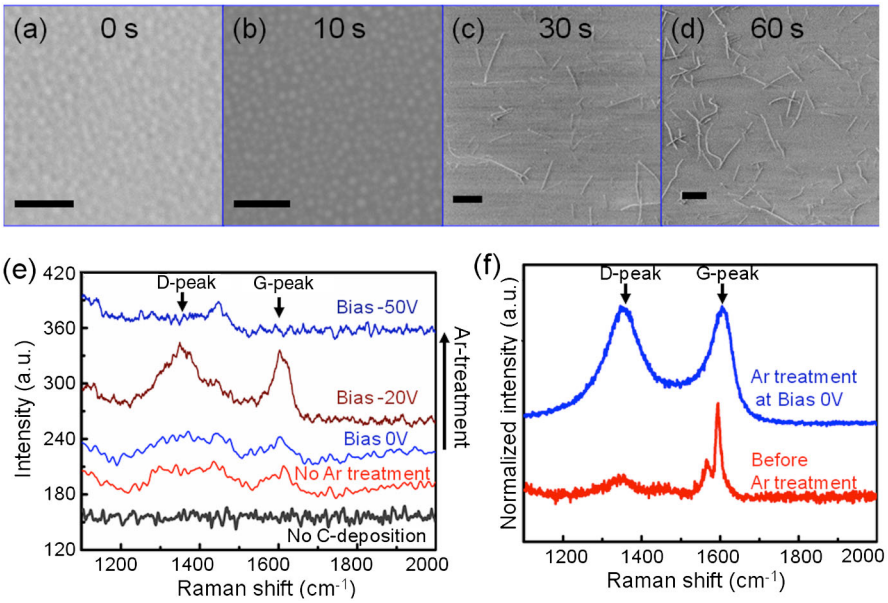

FIG. 3 (color online). Experimental observations of ion bombardment on the nascent SWCNT. (a)–(d) SWCNTs grown at 0, 10, 30, and 60 s, respectively. Scale bars in (a) and (b) are 200 nm and in (c) and (d) are 1 μm. (e) Raman spectra of 10 s growth SWCNTs with Ar ion bombardments at 0, −20, and −50 V biases. The graphitic *G* peak is most prominent at −20 V bias. (f) Raman spectra of 30 s growth SWCNTs before and after Ar ion bombardments at 0 V bias.

applied bias based on the experiments of Gahan *et al.* [37]. These authors found that with the increase in pressure not only the ion energy peak shifted to a lower value but also the ion distribution curve acquired a notable "tail" in the lower energy range. The ion energy peak at 50 mTorr pressure was found near ~6.6 eV (see Fig. S1 in the Supplemental Material [32]). Therefore, at a significantly higher pressure (100 mTorr as in our experiments), the ion energy peak can be expected to shift to a value of the order of ~4–5 eV due to the increased ion-neutral collisions. When the ions are extracted by applying an external bias, the ion energy gain is lower than the value of the applied substrate bias due to the ion-neutral collisions [38].

The ion energy gain (due to the ion extractor system) is therefore expected to be lower than the applied biases of 20 and 50 V. The corresponding peak ion energies at the substrate could thus be estimated to be in the ~18–22 eV range in the case of the applied bias of 20 V. As substantiated above, this energy is sufficient for displacing and removing undercoordinated C atoms, but below the threshold for C displacements from the graphene lattice positions (see also Sec. S3 in the Supplemental Material [32]). When a 50 V bias is applied, the peak ion energy could be reasonably expected in the ~45–48 eV range, which is in any case above the carbon displacement threshold. These experimental results are consistent with the preceding theoretical analysis of the effects of ion impact on carbon atom networks.

Finally, it is worth mentioning that the process of collision-induced network restructuring at low energies might at first glance seem to be similar to the process of temperature-induced annealing. However, two important differences should be considered. First, while thermal annealing delivers a global energy input, the energy input due to the Ar bombardment is very local. Indeed, when the Ar ion impinges on the network, essentially only the targeted C atom and its immediate surroundings are temporarily heated. If the energy transferred by the impinging ion is lower than the bond breaking energy threshold, there is no effect on the carbon network. If this energy is higher than the energy needed to physically displace and remove C atoms from the network in addition to breaking of one or several C-C bonds, then the network will be destroyed. If, however, the transferred energy is between the bond breaking energy threshold and the carbon displacement energy, bond breaking occurs, leading to the formation of new bonds in the network. Thus, in this case, the restructuring of the network is impact induced, and this leads to growth of the network.

Second, thermal annealing acts on both the carbon network and on the nickel cluster. Both the nickel cluster and the carbon network are heated, and in order to induce sufficient restructuring of the network, a high temperature is required, precluding a solid catalyst. Ion bombardment, on the other hand, acts in first instance only on the carbon network. Therefore, this possibly allows the catalyst particle to remain solid, which may be beneficial for catalyst morphology directed growth.

In conclusion, we combined atomic scale simulations with dedicated experiments in order to elucidate the influence of ion bombardment on CNT nucleation. While simulations and experiments typically address very different time and length scales, the experiments were designed to mimic the simulation conditions as closely as possible.

Using this approach, we demonstrated that ion bombardment may enhance carbon nanotube nucleation, provided that the ion energy is controlled in a specific energy window, which is determined by the intrinsic properties of atomic networks in the nanotubes. This may open new avenues for the effective nonthermal control over SWCNT growth.

The authors gratefully acknowledge financial support from the Prime Minister's Office through IAP VI. This work was carried out in part using the Turing HPC infrastructure at the CalcUA core facility of the Universiteit Antwerpen, a division of the Flemish Supercomputer Center VSC, funded by the Hercules Foundation, the Flemish government (department EWI), and the Universiteit Antwerpen. A. C. T. v. D. gratefully acknowledges the support provided by the U.S. Air Force Office of Scientific Research (AFOSR), Grant No. FA9550-11-1-0158. This work was partially supported by the Australian Research Council and CSIRO's OCE Science Leadership Program.

*Corresponding author.
erik.neyts@ua.ac.be

[1] R. A. Harutyunyan, G. G. Chen, T. M. Paronyan, E. M. Pigos, O. A. Kuznetsov, K. Hewaparakrama, S. M. Kim, D. Zakharov, E. A. Stach, and G. U. Sumanasekera, Science **326**, 116 (2009).
[2] S. M. Bachilo, L. Balzano, J. E. Herrera, F. Pompeo, D. E. Resasco, and R. B. Weisman, J. Am. Chem. Soc. **125**, 11186 (2003).
[3] Z. Ghorannevis, T. Kato, T. Kaneko, and R. Hatakeyama, J. Am. Chem. Soc. **132**, 9570 (2010).
[4] W.-H. Chiang and M. R. Sankaran, Nat. Mater. **8**, 882 (2009).
[5] M. F. C. Fiawoo, A. M. Bonnot, H. Amara, C. Bichara, J. Thibault-Penisson, and A. Loiseau, Phys. Rev. Lett. **108**, 195503 (2012).
[6] K. Toshiaki and R. Hatakeyama, ACS Nano **4**, 7395 (2010).
[7] Y. Ohta, Y. Okamoto, S. Irle, and K. Morokuma, ACS Nano **2**, 1437 (2008).
[8] E. C. Neyts, A. C. T. van Duin, and A. Bogaerts, J. Am. Chem. Soc. **133**, 17225 (2011).
[9] R. H. Baughman, A. A. Zakhidov, and W. A. de Heer, Science **297**, 787 (2002).
[10] A. Vijayaraghavan, F. Hennrich, N. Sturzi, M. Engel, M. Ganzhorn, M. Oron-Carl, C. W. Marquardt, S. Dehm, S. Lebedkin, M. M. Kappes, and R. Krupke, ACS Nano **4**, 2748 (2010).
[11] F. Ding, R. A. Harutyunyan, and B. Yakobson, Proc. Natl. Acad. Sci. U.S.A. **106**, 2506 (2009).
[12] R. Rao, D. Liptak, T. Cherukuri, B. I. Yakobson, and B. Maruyama, Nat. Mater. **11**, 213 (2012).
[13] G. Zhang, P. Qi, X. Wang, Y. Lu, X. Li, R. Tu, S. Bangsaruntip, D. Mann, L. Zhang, and H. Dai, Science **314**, 974 (2006).
[14] K. K. K. Koziol, C. Ducati, and A. H. Windle, Chem. Mater. **22**, 4904 (2010).
[15] S. Reich, L. Li, and J. Robertson, Chem. Phys. Lett. **421**, 469 (2006).
[16] N. Ishigami, H. Ago, K. Imamoto, M. Tsuji, K. Iakoubovskii, and N. Minami, J. Am. Chem. Soc. **130**, 9918 (2008).
[17] H. W. Zhu, K. Suenaga, J. Q. Wei, K. L. Wang, and D. H. Wu, J. Cryst. Growth **310**, 5473 (2008).
[18] D. A. Gomez-Gualdron, J. Zhao, and P. B. Balbuena, J. Chem. Phys. **134**, 014705 (2011).
[19] M. Diarra, H. Amara, C. Bichara, and F. Ducastelle, Phys. Rev. B **85**, 245446 (2012).
[20] K. Ostrikov and H. Mehdipour, J. Am. Chem. Soc. **134**, 4303 (2012).
[21] A. V. Krasheninnikov and F. Banhart, Nat. Mater. **6**, 723 (2007).
[22] Z. Q. Luo, S. H. Lim, Y. M. You, J. M. Miao, H. Gong, J. X. Zhang, S. Z. Wang, J. Y. Lin, and Z. X. Shen, Nanotechnology **19**, 255607 (2008).
[23] A. Gohier, T. M. Minea, A. M. Djouadi, A. Granier, and M. Dubosc, Chem. Phys. Lett. **421**, 242 (2006).
[24] M. Koster and H. M. Urbassek, Phys. Rev. B **63**, 224111 (2001).
[25] X. W. Zhang, H. G. Boyen, N. Deyneka, P. Ziemann, F. Banhart, and M. Schreck, Nat. Mater. **2**, 312 (2003).
[26] E. C. Neyts, A. C. T. van Duin, and A. Bogaerts, J. Am. Chem. Soc. **134**, 1256 (2012).
[27] H. J. C. Berendsen, J. P. M. Postma, W. F. van Gunsteren, A. DiNola, and J. R. Haak, J. Chem. Phys. **81**, 3684 (1984).
[28] A. C. T. van Duin, S. Dasgupta, F. Lorant, and W. A. Goddard III, J. Phys. Chem. A **105**, 9396 (2001).
[29] E. C. Neyts, Y. Shibuta, A. C. T. van Duin, and A. Bogaerts, ACS Nano **4**, 6665 (2010).
[30] R. Smith, in *Atomic and Ion Collisions in Solids and at Surfaces* (Cambridge University Press, Cambridge, England, 2005), p. 46–49.
[31] Z. J. Han and K. Ostrikov, J. Am. Chem. Soc. **134**, 6018 (2012).
[32] See Supplemental Material at http://link.aps.org/supplemental/10.1103/PhysRevLett.110.065501 for simulation details, ion energy distributions in similar plasma systems, recoil spectra of carbon and nickel atoms, experimental details, simulation movies, and additional references.
[33] O. Lehtinen, J. Kotakoski, A. V. Krasheninnikov, A. Tolvanen, K. Nordlund, and J. Keinonen, Phys. Rev. B **81**, 153401 (2010).
[34] G. L. Montet and G. E. Myers, Carbon **9**, 179 (1971).
[35] F. Banhart, Rep. Prog. Phys. **62**, 1181 (1999).
[36] A. V. Krasheninnikov, F. Banhart, J. X. Li, A. S. Foster, and R. M. Nieminen, Phys. Rev. B **72**, 125428 (2005).
[37] D. Gahan, B. Dolinaj, and M. B. Hopkins, Rev. Sci. Instrum. **79**, 033502 (2008).
[38] O. V. Vozniy, B. J. Park, K. S. Min, and G. Y. Yeom, J. Korean Phys. Soc. **50**, 1271 (2007).